

LiM 2011

Influence of the Pulse Duration in the ps-Regime on the Ablation Efficiency of Metals

B. Jaeggi*, B. Neuenschwander, M. Schmid, M. Mural, J. Zuercher and U. Hunziker

Applied Laser, Photonics and Surface Technologies, Bern University of Applied Sciences, Pestalozzistrasse 20, CH-3400 Burgdorf, Switzerland

Abstract

Ablation characteristics of copper and stainless steel with laser pulses from 10 to 100 ps at 1064 nm wavelength were studied. The influence of the pulse duration and the number of pulses on the threshold fluence and the penetration depth has been investigated. The results show a strong decrease of the ablation efficiency and quality with increasing pulse duration.

Keywords: Ablation characteristics; metals; picosecond laser pulses; threshold fluence; penetration depth; volume ablation rate

1. Introduction

For laser micro processing two different regions of pulse durations are used. The first region has typically pulse durations of nanoseconds and generates a heat affected zone in the material. The pulse duration is longer than the thermalization time of most metals [1] and is especially suitable for efficiently removing materials. On the other hand for high precision micro machining, ultrashort laser pulses with pulse durations typically in the region of 10 ps or less are preferable, as they show better results [2-5]. Laser systems generating pulse durations of 10 ps or less are more cost intensive than the systems with longer pulses. More and more laser systems with pulse durations in the range between these two regions are in development. One possibility are fiber based systems which are more cost effective than the ultrashort pulsed systems. These fiber based systems are expected to have pulse durations of several tenths of ps which exceed the thermalization time of most metals. In opposite to the two above mentioned regions of pulse durations, where a lot of results can be found in literature, the region between 10 ps and 100 ps are hardly investigated. Therefore this paper reports on applicability of laser pulses with pulse durations between 10 ps and 100 ps for the micromachining of copper and stainless steel.

2. Theoretical background

2.1. Threshold fluence and penetration depth

For describing the ablation process one of the important parameter is the thermalization time describing the photon-phonon coupling. For metals this thermalization time is estimated to be in the region of picoseconds [1]. In

* Corresponding author. Tel.: +41-34-4264193; Fax: +41-34-4231513.

E-mail address: beat.jaeggi@bfh.ch

the case of pulse durations shorter than the thermalization time there exists a two-temperature-model as discussed in [4-8]. As a consequence of this model the logarithmic law between the fluence F of the laser pulse and the ablation depth z_{abl} is given by [2, 4, 5]:

$$z_{abl} = \delta \cdot \ln(F/F_{th}) \quad (1)$$

According to equation (1) the ablation depth z_{abl} depends on the two material parameters penetration depth δ and threshold fluence F_{th} . The threshold fluence F_{th} describes the minimum energy which is needed to ablate material. The penetration depth δ is the ability of the energy to penetrate into the material. Additionally, according to J. M. Liu [9], there is a correlation between the threshold fluence F_{th} and the diameter D of the ablated crater as given by:

$$D^2 \propto \ln(F/F_{th}) \quad (2)$$

In general material ablation multiple pulses are fired on the same spot. Each pulse modifies the surface and therefore the surface property changes from pulse to pulse (incubation effect). According to [10-14] the relation between the threshold fluence F_{th} per pulse and the number of applied pulses N is given by:

$$F_{th} = F_{th}(1) \cdot N^{S-1} \quad (3)$$

where $F_{th}(1)$ is the threshold fluence of one pulse and S the incubation factor. If $S=1$ no incubation will appear. For values between 0 and 1, the material is softening and for values above 1 is hardening. For metals the factor S is typically between 0 and 1, meaning the threshold fluence decreases with increasing number of pulses. According to equation (3) for an infinite number of pulses the ablation threshold becomes zero. This is physically not possible. It is more likely, that with an infinite number of pulses the threshold fluence approaches a non-zero minimum value. Therefore with increasing number of pulses equation (3) becomes less accurate. In the investigated range of 1 to 512 pulses the equation (3) is applicable.

2.2. Volume ablation rate

In most industrial applications the ablation efficiency is essential and can be described with the ablated volume per time dV/dt . With the equation (1) and assuming a Gaussian beam profile the volume ablation rate can be written as a function of the repetition rate f and the average power P_{av} [15, 16]:

$$\frac{dV}{dt} = \frac{1}{4} \cdot \pi \cdot w_0^2 \cdot \delta \cdot f \cdot \ln^2 \left(\frac{2 \cdot P_{av}}{f \cdot \pi \cdot w_0^2 \cdot F_{th}} \right) \quad (4)$$

where δ and F_{th} are the two material parameters penetration depth and threshold fluence and w_0 the spot radius. Plotting the volume ablation rate as a function of the repetition rate f there exists a maximum volume ablation rate

$$\left(\frac{dV}{dt} \right)_{\max} = \frac{2}{e^2} \cdot \frac{\delta}{F_{th}} \cdot P_{av} \quad (5)$$

at an optimum repetition rate

$$f_{opt} = \frac{2}{e^2} \cdot \frac{1}{\pi \cdot w_0^2 \cdot F_{th}} \cdot P_{av} \quad (6)$$

3. Experimental Setup

In most industrial applications the process efficiency directly scales with the ablated volume per time dV/dt . The goal of our experiments was therefore to investigate the influence of the pulse duration (between 10 ps and 100 ps) and the number of applied pulses on the material parameters threshold fluence and penetration depth which directly scale the volume ablation rate (4).

As a source for the laser pulses a Duetto (Time Bandwidth Products) generating 10 ps pulses at 1064 nm wavelength was used. With the installation of significant etalons in the seed laser, pulse durations of 20 ps, 30 ps, 50 ps and 100 ps could be achieved. The pulse durations have been measured with an autocorrelator. The value of the repetition rate is ranging from 50 kHz up to 1 MHz. With a pulse picker it was possible to reduce the repetition rate down to single pulses. The average output power is up to 10 W. The laser beam was circular polarized by a $\lambda/4$ -plate and directed through two mirrors and a beam expander with two lenses onto the galvoscaner. With a 160 mm f-theta objective the beam is focused to a spot radius w_0 of 17.5 μm , which measured with a slit scanning beam profiler. The same measurement showed a laser beam quality of $M^2 \leq 1.3$ and therefore the beam can be assumed to be Gaussian shaped. The pulse durations had no influence on the laser beam parameters.

All experiments were performed with the target surface in the focal plane of the f-theta objective. In order to exclude heat accumulation the experiments for measuring the ablation threshold and the penetration depth were performed with 50 Hz repetition rate. The average power was set up previously at a repetition rate of 50 kHz.

Multiple craters with different applied fluences and number of pulses were produced. The crater depth and the crater diameter were determined with a Laser Scanning Microscope LSM. The values for the threshold fluence and the penetrations depth were obtained with a least square fit according to equation (1). The threshold fluence was also be deduced by using the crater diameter and equation (2). Both methods lead to comparable results for the threshold fluence whereas the penetration depth can only be obtained with the first method.

To determine the volume ablation rate dV/dt , lines at a fixed average power, repetition rate and pulse duration, but different scanner speed v and different iterations, were ablated. The volume of the ablated line dV/dt_{line} was again measured with the LSM. Together with the scanner speed the volume ablation rate was calculated.

Additionally the roughness of the ablated lines was measured in the middle of the lines with the Laser Scanning Microscope. We measured the arithmetical mean roughness R_a and the ten-point mean roughness R_z .

The analyzed materials were copper Cu-DHP (in US: C12 200) and stainless steel 1.4301 (in US: AISI 304) whose surfaces were polished with a diamond suspension.

4. Results and Discussion

4.1. Dependency of the threshold fluence and the penetration depth on the number of pulses

The dependency of the threshold fluence on the number of pulses has been investigated. The ablation depth was measured for different number of pulses and different fluences applied with these pulses. Figure 1a shows the measured threshold fluence for copper and steel for the pulse durations 10 ps and 50 ps, respectively. It is clearly

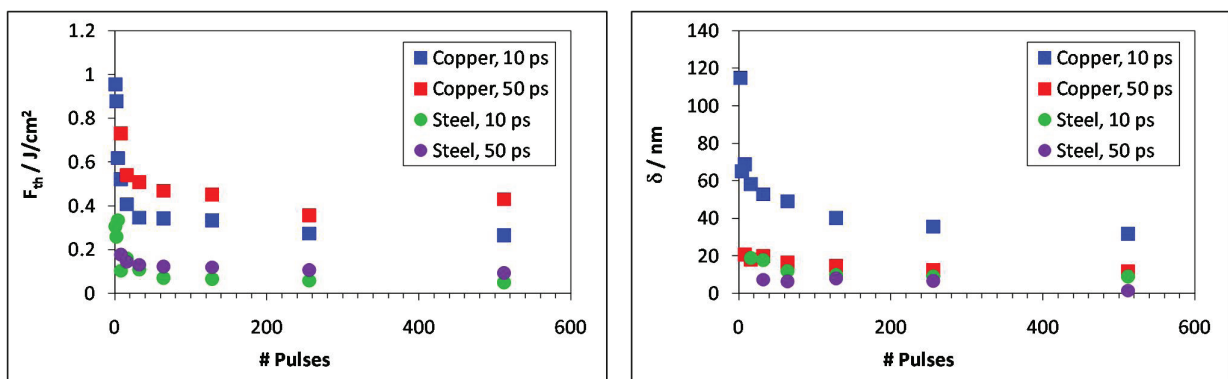


Figure 1. (a) Threshold fluence versus number of pulses for copper and steel, 10 and 50 ps; (b) Penetration depth versus number of pulses for copper and steel, 10 and 50 ps

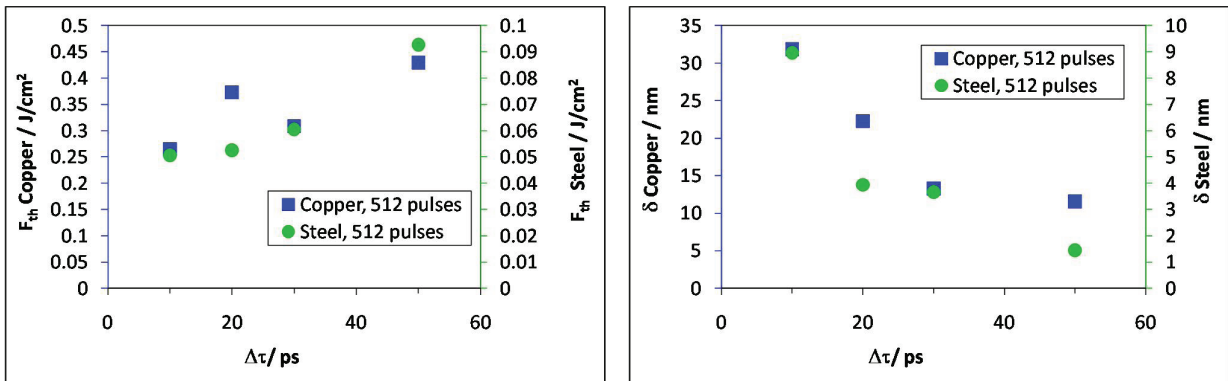


Figure 2. (a) Threshold fluence versus pulse duration for copper and steel, 512 applied pulses; (b) Penetration depth versus pulse duration for copper and steel, 512 applied pulses

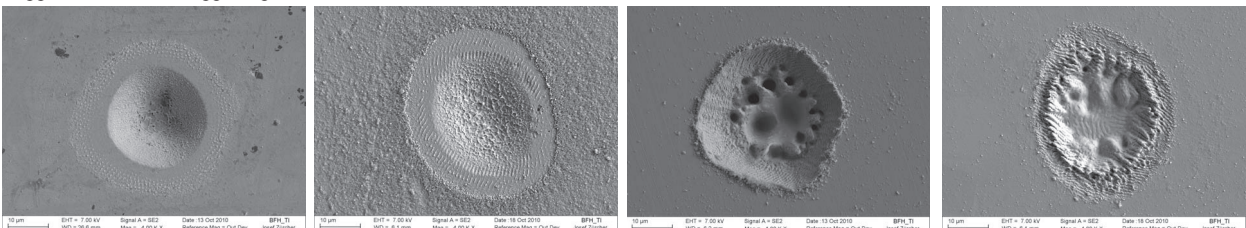


Figure 3. (a) SEM picture of the ablated crater in copper, 10 ps 1.45 J/cm^2 peak fluence and 256 pulses; (b) in copper 50 ps; (c) ablated crater in steel 10 ps 1.81 J/cm^2 peak fluence 256 pulses; (d) in steel 50 ps

seen that the threshold fluence decrease with increasing number of pulses according to equation (3). For 10 ps and 1 pulse the threshold fluence is 0.95 J/cm^2 for copper, 0.31 J/cm^2 for steel, and goes down to 0.27 J/cm^2 for copper and 0.05 J/cm^2 for steel (for 512 pulses). The accumulation factor S is for copper in the range of 0.79 for 10 ps to 0.87 for 50 ps, 0.7 and 0.87 for stainless steel, respectively. Therefore a softening of the material occurs. Our results confirm to the results of [11, 12, 14].

Figure 1b shows the dependency of the penetration depth on the applied number of pulses. The penetration depth was estimated by a least square fit with equation (1). The penetration depth also decreases with higher number of pulses. The penetration depth for 10 ps and copper goes down from 114.9 nm at 2 pulses to 31.8 nm at 512 pulses, for steel from 18.8 nm at 16 pulses down to 11.6 nm at 512 pulses. Because of the small depth of the crater, it was not possible to determine the penetration depth for the lower numbers of applied pulses.

The decrease of the two material parameters with increasing number of pulses can be explained by local material transformation [10, 13] and the change of the surface reflectivity due to oxidation and increased surface roughness from pulse to pulse.

4.2. Dependency of the threshold fluence and the penetration depth on the pulse duration

Figure 2 shows the dependency of the two material parameters threshold fluence and penetration depth on the pulse duration for copper and steel. The threshold fluence increases with longer pulse durations. For 10 ps and 512 pulses we have a threshold fluence of 0.27 J/cm^2 for copper and 0.05 J/cm^2 for steel. This rate increases to 0.43 J/cm^2 for copper and 0.09 J/cm^2 for steel for 50 ps. The penetration depth strongly decreases with increasing pulse duration: For copper from 31.8 nm for 10 ps, down to 11.6 nm for 50 ps (for 512 pulses), for steel from 9 nm for 10 ps down to 1.44 nm for 50 ps, respectively. The influence of the pulse duration on the threshold fluence and the penetration depth is strong. According to [6] hydrodynamic plasma expansion during the laser pulse, plasma shielding of the laser radiation and increased heat-conduction loss are possible reasons for the above mentioned behavior. However the surprisingly decrease of δ with the pulse duration is not fully understood and is subject of ongoing investigations.

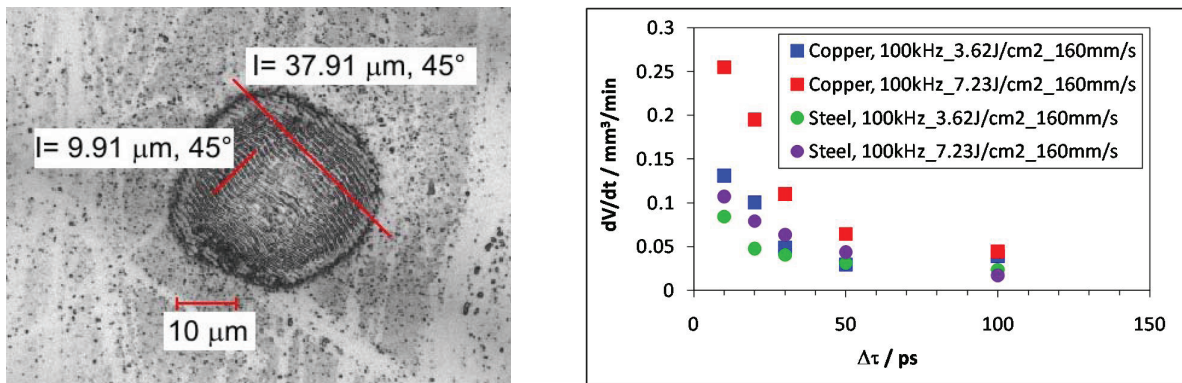


Figure 4. (a) Ripples orientation and distance in steel, 10 ps 1.45 J/cm^2 peak fluence 32 pulses; (b) Volume ablation rate at constant fluence versus pulse duration

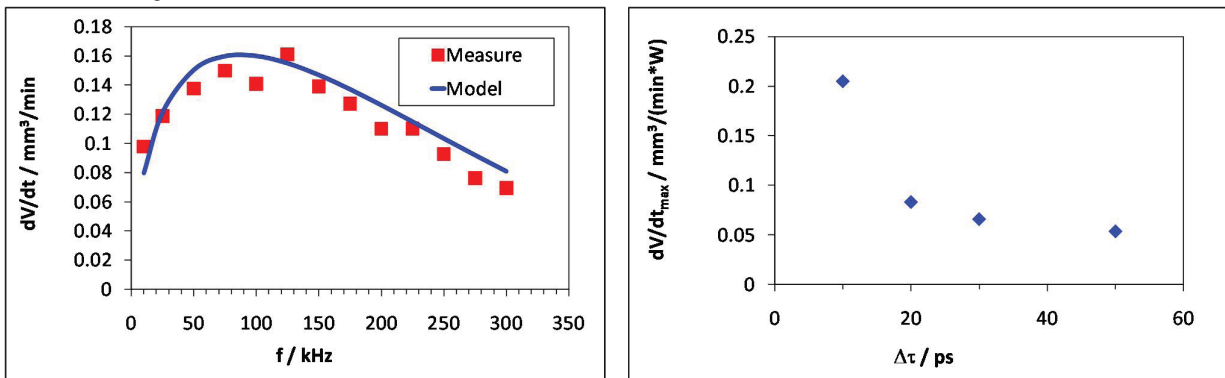


Figure 5. (a) Comparison between the theoretical model and the measurement for 10 ps 3.62 J/cm^2 peak fluence; (b) Calculated maximum volume ablation rate per average power versus pulse duration for copper

4.3. Quality of the ablated crater

In the case of steel it was very difficult to measure the ablation depth because of the melted material in the crater. Figures 3a,b shows an ablated crater with 1.45 J/cm^2 peak fluence and 256 pulses in copper for 10 ps and 50 ps. Figures 3c,d shows an ablated crater with 1.81 J/cm^2 peak fluence and 512 pulses in stainless steel. In the case of copper with 10 ps a nearly smooth crater surface can be observed (Figure 3a). The cross section of the crater reveals an parabolic shape. On the other hand for a pulse duration of 50 ps some melted material is observed in the crater (Figure 3b). In the case of steel already for 10 ps the shape of the cross section is no more parabolic and the crater is filled with melted material (Figure 3c). The effect is even more prominent for 50 ps (Figure 3d).

An interesting observation are ripples observed within the ablation crater (Figure 4a). These ripples have an angle of approximately 45° to the horizontal line and are caused by the circular polarization of the laser. As shown in Figure 4a the distance between ten succeeding ripples is $9.91 \mu\text{m}$. Therefore the distance between two ripples is approximately the wavelength of the incoming light [10, 13, 17].

4.4. Volume ablation rate

This measure was experimentally deduced from single lines, generated with different pulse durations and fluences. Figure 4b shows the dependency of the volume ablation rate for two different fluences for copper and steel, respectively. The volume ablation rate strongly decreases with longer pulse durations. Choosing 7.23 J/cm^2 peak fluence, 100 kHz repetition rate and a scanner speed of 160 mm/s the volume ablation rate for copper goes

down from $0.25 \text{ mm}^3/\text{min}$ for 10 ps to $0.04 \text{ mm}^3/\text{min}$ for 100 ps, for steel from $0.11 \text{ mm}^3/\text{min}$ to $0.02 \text{ mm}^3/\text{min}$. This is a consequence of the dependency from the pulse duration of the threshold fluence and the penetration depth as discussed in section 4.2. At the fixed average power and repetition rate, no differences of the volume ablation rate in respect of the different scanner speeds are detected.

To verify the model for the volume ablation rate, see equation (4), the volume ablation rate in function of the repetition rate was determined. If we use in equation (4) the previously determined material parameters, it is possible to calculate the volume ablation rate. Note that the correct number of pulses per area has to be calculated. There is a good agreement between the model function and the experiment as seen in Figure 5a. As mentioned in section 2.2 an optimum volume ablation rate exists at an optimum repetition rate. This repetition rate depends on the threshold fluence, which itself is depending on the pulse duration as shown in Figure 2a. Therefore the optimum repetition rate depends on the pulse duration, as well. Because of the increasing threshold fluence with increasing pulse duration, the optimum repetition rate decrease with increasing pulse duration.

Assuming a system is optimized for a maximum efficiency, an optimum repetition rate instead of a fixed repetition rate will be used. In this way it is possible to compare at the maximum volume ablation rate, as seen in Figure 5b. These values are calculated with the correct threshold fluence and penetration depth for the number of pulses each spot sees and are not measured. As the threshold fluence increases and the penetration depth decreases with increasing pulse duration the observed drop of the maximum volume ablation rate is even more pronounced, compared to Figure 4b. The maximum volume ablation rate for copper goes down from $0.2 \text{ mm}^3/(\text{min} \cdot \text{W})$ for 10 ps to $0.05 \text{ mm}^3/(\text{min} \cdot \text{W})$ for 50 ps.

4.5. Quality of the ablated lines

For a complete comparison also the quality of the ablated lines has to be taken into account, as well.

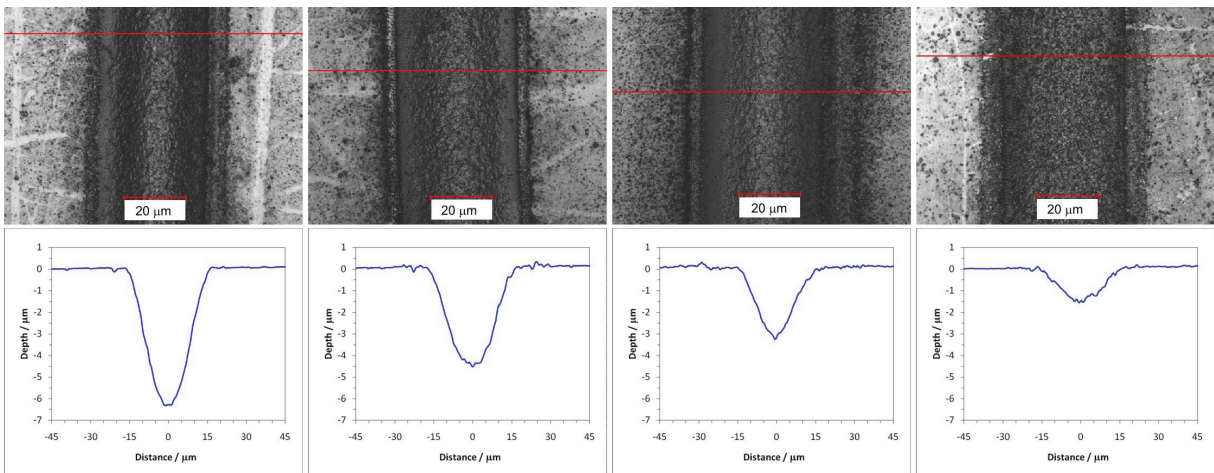


Figure 6. (a) Top view and profile of a line for copper, 10 ps 3.62 J/cm^2 100 kHz 160 mm/s; (b) 20 ps; (c) 30 ps; (d) 50 ps

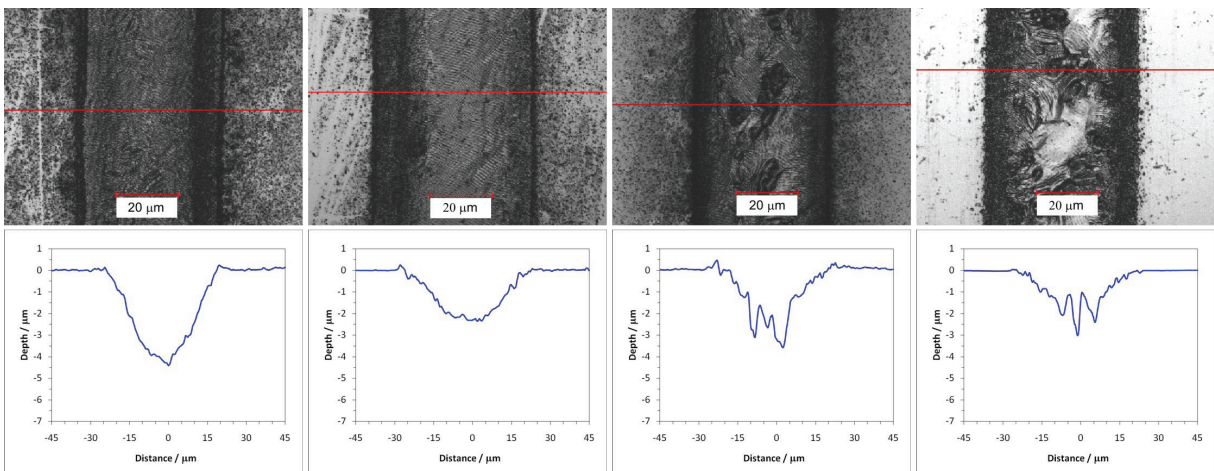


Figure 7. (a) Top view and profile of a line for steel, 10 ps 3.62 J/cm^2 100 kHz 160 mm/s; (b) 20 ps; (c) 30 ps; (d) 50 ps

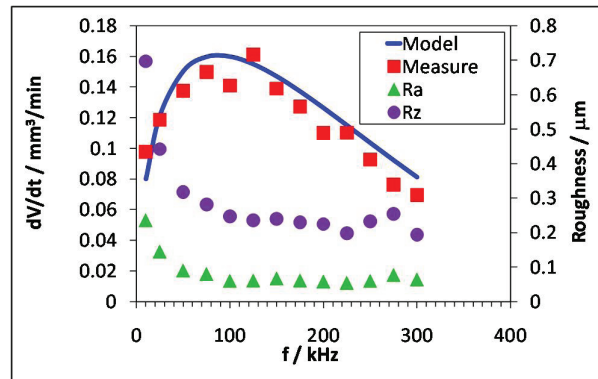


Figure 8. Roughness versus the repetition rate, copper 10 ps, 3.62 J/cm²

In Figures 6 and 7 typical results of the top views and the profiles of the lines in copper and steel are shown for 10, 20, 30 and 50 ps. Profiles in copper are close to a parabolic shape, expected from the logarithmic ablation law of equation (1). In the case of 50 ps melted material is observed in the middle of the groove, and the groove surface is rough. In contrast for steel melted material is observed in the line even at pulse durations of 10 ps, see Figure 7a; this effect increases with the pulse duration. From this point of view the ablation of steel is not free of a melting zone for 10 ps. For 30 ps and 50 ps we can not detect a clear dike as for 10 ps. In the top views in the case of steel, the melting zone is clearly visible at 30 and 50 ps. In the case of copper we see more debris around the line at the higher pulse durations as for 10 ps. For both materials for a well defined ablation shorter pulse durations are favorable.

Another possibility to get some information about the quality is to determine the roughness of the lines. The roughness was determined for the different repetition rates of the model of the volume ablation rate. In Figure 8 it can be seen, that the roughness is increasing for small repetition rates. At the optimum point for the ablation (87 kHz), the roughness is almost as large as at high repetition rates. From about 70 kHz the roughness R_a , and from 100 kHz the roughness R_z , are constant at the values 0.08 μm and 0.25 μm , respectively. The roughness of the ablated lines is depends on a few parameters, such as the depth of the lines, the fluence, the iterations, the pulse duration etc. Therefore it is difficult to show only the influence of the pulse duration. The best values of the arithmetical mean roughness are less than 100 nm.

5. Comparing the results with other pulse durations

At the moment our setup does not allow to expand our experiments to higher and smaller pulse durations. Also there exist values for the threshold fluence in the literature for pulses with durations in the range of a few fs and more [5, 12, 18, 19] a direct estimation of the volume ablation rate becomes difficult. Mostly the number of pulses, used to determine the parameters, is not known and the value of the penetration depth which is used to deduce the maximum volume ablation rate with equation (5) is missing. Furthermore the experiments are often performed at a wavelength around 800 nm which differs from the 1064 nm used in our experiments. A brief estimation based on published values show a much higher volume ablation rate in the regime of several 10 ns and comparable volume ablation rates in the range of 100 fs. However, due to the mentioned uncertainties the range between 500 fs and 10 ps has to be investigated with tailored experiments.

6. Summary and Outlook

We have shown that in the regime from 10 ps to 100 ps for stainless steel and copper the threshold fluence and the penetration depth depends on the number of applied pulses and the pulse duration, as well. The results for the dependence on the number of applied pulses correspond to [11], also for pulse durations higher than 10 ps. The simultaneous increase of the threshold fluence and decrease of the penetration depth for higher pulse duration lead to a significant drop of the maximum volume ablation rate. The shape of this maximum volume ablation rate as a

function of the pulse duration indicates that pulses shorter than 10 ps are preferable. It can be assumed that other metals will also show the similar behavior. For treating metals new laser systems with pulse durations higher than 10 ps must therefore show other advantages in order to be competitive. In contrast, for other materials the characteristics could differ and therefore have to be verified. Additional investigations will be done in future, also to determine the maximum volume ablation rate in the crossover between femto- and picoseconds.

References

- [1] Hirayama Y., Obara M.: Heat-affected zone and ablation rate of copper ablated with femtosecond laser, *J. of Appl. Phys.* 97, 064903 (2005)
- [2] Momma C., Chichkov B.N., Nolte S., von Alvensleben F., Tünnermann A., Welling H. et al.: Short-pulse laser ablation of solid targets, *Opt. Commun.* 129 (1996) 134-142
- [3] Liu X., Du D., Mourou G.: Laser Ablation and Micromachining with Ultrashort Laser Pulses, *IEEE J. of Quan.electr.* vol. 33 No. 10 oct. 1997
- [4] Chichkov B.N., Momma C., Nolte S., von Alvensleben F., Tünnermann A.: Femtosecond, picosecond and nanosecond laser ablation of solids, *Appl. Phys. A* 63 (1996) 109-115
- [5] Momma C., Nolte S., Chichkov B.N., v. Alvenleben F., Tünnermann A.: Precise laser ablation with ultrashort pulses, *Appl. Phys. Sci.* 109/110 (1997) 15-19
- [6] Nolte S., Momma C., Jacobs H., Tünnermann A., Chichkov B.N., Wellegehausen B. et al.: Ablation of metals by ultrashort laser pulses, *J. Opt. Soc. Am. B / Vol 14, No. 10 / October 1997*
- [7] Nolte S.: Mikromateriabearbeitung mit ultrakurzen Laserpulsen, Dissertation, Duvillier Verlag, Göttingen, 1999
- [8] Körner C.: Theoretische Untersuchungen zur Wechselwirkung von ultrakurzen Laserpulsen mit Metallen, Dissertation der technischen Fakultät der Universität Erlangen-Nürnberg, 1997
- [9] Liu J.M.: Simple techniques for measurements of pulsed Gaussian-beam spot sizes, *Opt. Lett.* 7, 196, 1982
- [10] Jee Y., Becker M.F., and Walser R.M.: Laser-induced damage on single-crystal metal surfaces, *J. Opt. Soc. Am.* B5, 1988
- [11] Raciukaitis G., Brikas M., Gecys P., Voisiat B., Gedvilas M.: Use of High Repetition Rate and High Power Lasers in Microfabrication: How to Keep the Efficiency High?, *JLMN journal of Laser Micro/Nanoengineering* Vol. 4 (3) 186 (2009)
- [12] Mannion P.T., Magee J., Coyne E., O'Connor G.M., Glynn T.J.: The effect of damage accumulation behavior on ablation thresholds and damage morphology in ultrafast laser micro-machining of common metals in air, *Appl. Surf. Sci.* 233 (2004) 275-287
- [13] Byskov-Nielsen J., Short-pulse laser ablation of metals: Fundamentals and applications for micro-mechanical interlocking, PhD thesis Department of Physics and Astronomy University of Aarhus Denmark, 2010
- [14] Kirkwood S.E., van Popta A.C., Tsui Y.Y., Fedosejevs R.: Single and multiple shot near-infrared femtosecond laser pulse ablation thresholds of copper, *Appl. Phys. A* 81 (2005) 729-735
- [15] Neuenschwander B., Bucher G., Hennig G., Nussbaum C., Joss B., Murali M., Zehnder S. et al.: Processing of dielectric materials and metals with ps laserpulses, Paper M101, ICALEO 2010
- [16] Neuenschwander B., Bucher G., Nussbaum C., Joss B., Murali M., Hunziker U. et al.: Processing of dielectric materials and metals with ps-laserpulses: results, strategies limitations and needs, *Proceedings of SPIE* vol. 7584 (2010)
- [17] Tan B., Venkatakrisnan K.: A femtosecond laser-induced periodical surface structure on crystalline silicon, *J. Micromech. Microeng.* 16 (2006) 1-6
- [18] Nedialkov N.N., Imamova S.E., Atanasov P.A.: Ablation of metals by ultrashort laser pulses, *J. Phys. D: Appl. Phys.* 37 (2004) 638-643
- [19] Mannion P., Magee J., Coyne E., O'Connor G.: Ablation thresholds in ultrafast laser micro-machining of common metals in air, *Proc. Of SPIE* Vol. 4876 (2003)